

Environmentally Friendly Production of Cellulose Nanofibers Using Laser-Assisted Lignocellulose Decomposition

Leo Adachi, Shuhei Yamada, Shun-ichi Ishiuchi, and Hiroyuki Wada*

Institute of Science Tokyo, 4259 Nagatsuta, Migori-ku, Yokohama, Kanagawa 226-8503, Japan

**Corresponding author's e-mail: Wada.h.ac@m.titech.ac.jp*

An eco-friendly approach for producing cellulose nanofibers (CNFs) through laser treatment of lignocellulose nanofibers (LCNFs) is presented. Traditional CNF production methods require large amounts of organic solvents. Additionally, these methods lack flexibility in adjusting the ratios of cellulose, hemicellulose, and lignin, necessitating ratio control during pulping, which can impact subsequent stages. In contrast, this method reduces solvent use significantly and allows control over lignin content by adjusting laser irradiation time. Analytical techniques, including UV-vis, ^{13}C NMR, SEM, and XRD confirmed that laser treatment selectively decomposes lignin and other xylan residues while maintaining CNF structure. This method offers a promising, sustainable alternative for CNF production with notable environmental benefits

DOI: 10.2961/jlmn.2025.02.2004

Keywords: cellulose nanofiber, CNF, lignocellulose nanofiber, LCNF, wood, photochemistry

1. Introduction

Wood comprises cellulose, hemicellulose, and lignin [1]. Cellulose nanofibers (CNFs) are produced by finely disentangling cellulose, the main component of wood. Nanofibers are defined as fibers with a width of 100 nm or less or as micro-sized fibers with nano-scale cross-sections [2]. CNFs offer numerous advantages, including a thermal expansion coefficient one-tenth that of glass [3] and a strength 25 times that of steel [4, 5]. Leveraging these properties, CNFs are expected to find applications across various fields. Examples of such applications include nanopaper for electronic devices [6-8], composite materials such as resins [9, 10], biocompatible materials for cosmetics and thickeners [11], and gas or oxygen barrier films [12]. Additionally, lignin and hemicellulose containing nanofibers derived directly from wood, known as lignocellulose nanofibers (LCNFs), exhibit unique properties absent in CNFs, such as high thermostability [13] and antimicrobial activity [14, 15]. Cellulose is a linear polymer of β -glucose, while hemicellulose has a branched structure of xylan, mannan, and other polysaccharides [16]. Lignin, an aromatic polymer, functions as a binder for wood cells [17].

Manufacturing CNFs from wood occurs in two stages. The first stage removes all components except cellulose, yielding cellulose pulp, which is then finely disentangled in the second stage to produce CNFs [2, 18-20]. Specific methods for producing CNFs include mechanical approaches such as the high-pressure homogenizer method, which involves disentangling cellulose fibers by forcing the material through narrow gaps under high pressure [21], and the water jet method, where a dispersion of the sample is collided to achieve fiber separation [22], and grinding methods using grinders [23]. Additionally, chemical methods like TEMPO oxidation, which modifies side chains to enhance fibrillation through intermolecular repulsion [2], and biological methods employing enzymes [24] have also been developed. These processes require substantial organic solvents, which impose a high environmental burden. Furthermore, the

current two-stage process involves adjusting the component ratios during the first stage, leaving no opportunity for further adjustment in the second stage. This limitation makes precise control of the component ratios inherently challenging.

This study proposes a method to manufacture LCNFs directly from wood and subsequently create CNFs by selectively removing lignin from the LCNFs. As a novel approach, light is considered for lignin removal, enabling detailed reaction control. This method could yield CNFs and LCNFs with tailored component ratios while reducing the required volume of organic solvents. The focus of this study is to analyze the effects of laser irradiation on wood components and evaluate the potential of this proposed approach.

2. Experimental methods

2.1 Preparation of materials

In this study, the optical properties of specific materials were evaluated, including cellulose, xylan (the main component of hemicellulose) extracted from cone core, and lignin. Three types were selected for lignin: alkaline lignin, dealkaline lignin, and sodium lignin sulfonate.

Additionally, xylan, CNF, and LCNF were included for both before and after laser evaluations. Each material was measured at 1g and prepared by dissolving or dispersing it in 20 to 30 mL of aqueous solution. A 3 mL from each solution was used as a sample for each experiment.

2.2 Laser irradiation conditions

Nd: YAG laser's third harmonic (355 nm) was chosen as the light source due to its appropriate energy level for the desired excitation. A schematic diagram of the laser system is shown in Fig. 1. The laser irradiation conditions were defined with precision. The repetition rate was set at 20 Hz. The pulse width was controlled within the range of 4-6 ns and the laser diameter is 7-8 mm. Furthermore, the laser power was maintained between 6.5-130 mJ/cm² to ensure

sufficient energy delivery. The irradiation duration was either 0.5 h or 5 h, a span deemed suitable for observing any structural or molecular changes in the materials.

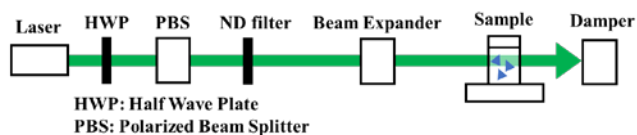


Fig. 1 A schematic diagram of the laser system.

2.3 Characterization and analysis

The first step in the analysis phase was to measure the diffuse reflectance spectra, allowing for an understanding of the optical properties inherent to each wood component. These measurements were performed using a UV-visible absorption spectrophotometer (UV-Vis), with the resulting data being transformed via Kubelka-Munk (K-M) conversion for more reliable analysis.

Subsequently, the samples were compared and evaluated to assess changes before and after laser irradiation. These evaluations spanned multiple parameters. Optical properties were analyzed using UV-Vis spectroscopy to observe any alterations in light absorption. Morphology was examined via scanning electron microscopy (SEM), providing high-resolution images to identify changes in the physical structure of the materials. Additionally, molecular binding was investigated using ^{13}C CP/MAS solid-state nuclear magnetic resonance (NMR), offering insights into shifts in molecular structures. Finally, crystallinity was evaluated through powder X-ray diffraction (XRD).

The crystallinity index was calculated using the widely applied Segal method [25], which evaluates the relative crystallinity of cellulose. This method employs the diffraction peak intensity corresponding to the crystalline (002) plane I_{002} and the minimum intensity between the (002) and amorphous peaks I_{am} , representing the height of the amorphous region.

$$\left(1 - \frac{I_{am}}{I_{002}}\right) \times 100. \quad (1)$$

By applying this approach, quantitative comparisons of crystallinity before and after laser irradiation were made to determine the extent of structural changes in the cellulose framework.

3. Results and discussions

3.1 Diffuse reflection spectra

Fig. 2 shows the diffuse reflection spectra results, with intensity values converted using the Kubelka-Munk (K-M) function. At wavelengths around 355 nm, cellulose shows minimal peaks, while xylan and lignin exhibit high K-M values, indicating absorption bands for xylan and lignin at this wavelength. This suggests that a 355 nm laser can selectively induce photochemical reactions in xylan and lignin without affecting cellulose. It is reported that cellulose undergoes photodegradation at wavelengths below 340 nm [26, 27], while lignin decomposes at wavelengths above 280 nm [28]. Therefore, the 355 nm laser may allow selective decomposition of non-cellulose components (xylan and lignin)

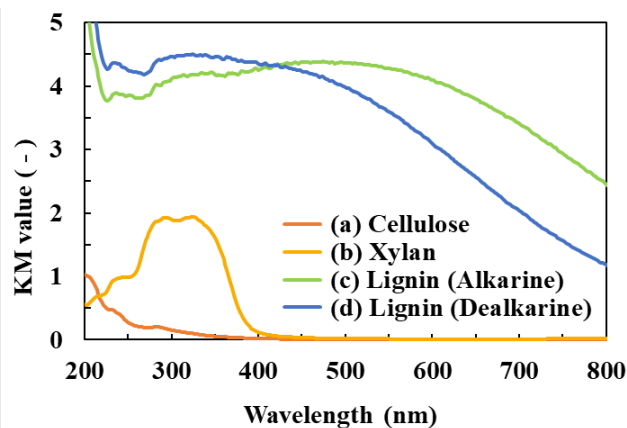


Fig. 2 The diffuse reflection spectra of wood components such as (a) Cellulose, (b) Xylan from cone, (c) Lignin (Alkarine), (d) Lignin (Dealkarine).

while preserving cellulose.

3.2 Xylan

Fig. 3 shows changes in the absorption spectra with varying laser fluence. The observed spectral peaks were assigned as follows [29-35]: the peak at 325 nm corresponds to cinnamic acid, which links hemicellulose and lignin. The peak at 290 nm is associated with cellulolytic enzyme lignin (CEL), a residual lignin component. Lastly, the peak at 230 nm is linked to hexuronic acid, derived from the side chain of xylan. These results indicate that laser treatment effectively decomposes lignin residues and xylan side chains present within xylan from cone core.

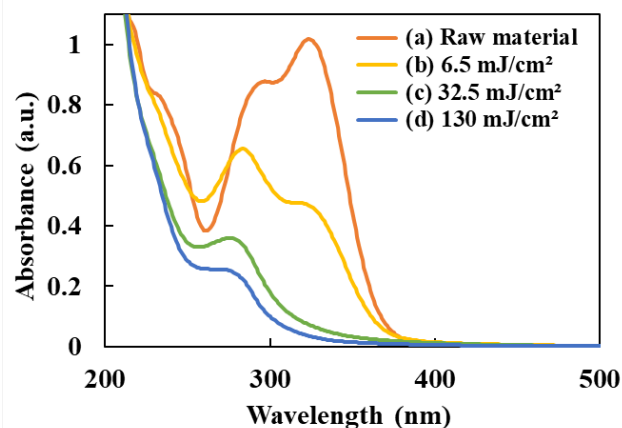


Fig. 3 The absorption spectra of xylan (a) before and after laser irradiation at fluence of (b) 6.5, (c) 32.5, (d) 130 mJ/cm².

3.3 CNF

Fig. 4 presents the SEM images of CNF before and after laser irradiation. The existence of nanofibers ranging in size from several tens to hundreds of nanometers was noted, with fibers interlacing to form a tangled structure. Despite laser irradiation, no morphological changes were observed in the CNF.

Subsequently, the results of the ^{13}C solid NMR measurements on the CNF before and after laser irradiation are

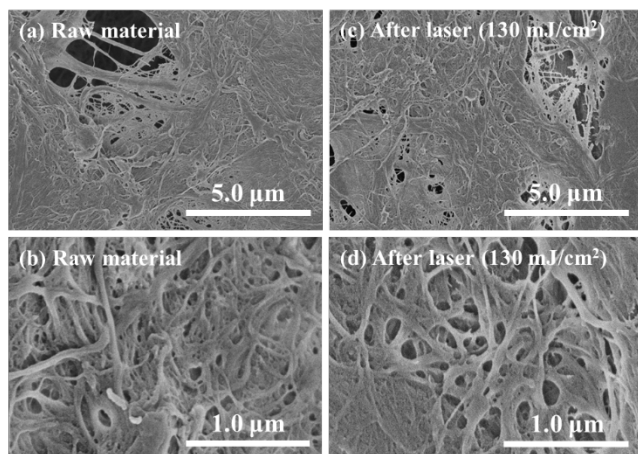


Fig. 4 SEM images of CNFs from raw material at (a) low and (b) high magnification, and after laser irradiation with 130 mJ/cm² at (c) low and (d) high magnification, respectively.

illustrated in Fig. 5. Peaks attributable to cellulose were found at 62 ppm for the C6 position (amorphous), 65 ppm for the C6 position (crystalline), 72–75 ppm for the C2, 3, 5 positions, 84 ppm for the C4 position (amorphous), around 89 ppm for the C4 position (crystalline), and near 105 ppm for the C1 position [36, 37]. Fig. 6 shows an enlarged view of the spectra in Fig. 4. Most peaks remained unchanged following laser irradiation. However, a slight broadening of the peaks at 72–75 ppm (C2, C3, C5 positions) and 84 ppm (amorphous C4 position) was noted, indicating potential minor structural changes in the cellulose due to laser treatment.

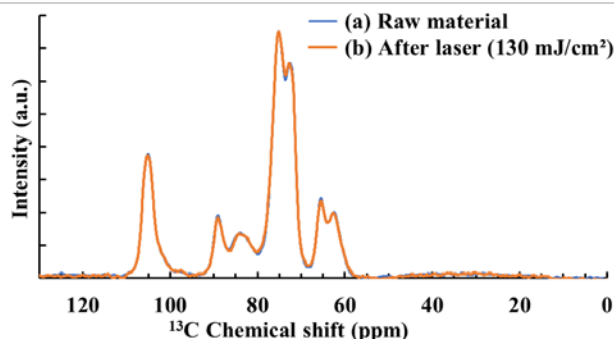


Fig. 5 ¹³C solid NMR of CNFs from (a) raw material and (b) after laser irradiation with 130 mJ/cm², respectively.

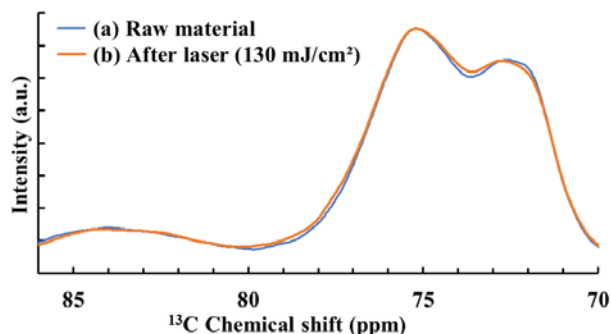


Fig. 6 An enlarged view of the spectra in Fig. 4.

Furthermore, the XRD measurement results for the CNF before and after laser irradiation are depicted in Fig. 7. The

diffraction patterns for the (200), (110), and (-110) planes remained consistent, suggesting that the cellulose I β structure was maintained. However, the crystallinity index slightly decreased from 63.1 to 59.3 after irradiation, supporting the ¹³C NMR results that suggested minor structural changes. Upon considering the results in Figures 4–7, it appears that laser irradiation preserved the morphology, bonding, and crystallinity of CNF with only minimal structural changes.

Prior studies have reported that although cellulose exposed to 532 nm light showed no chemical changes, long-term resistance was affected, and 1064 nm exposure led to an increase in polymerization due to intra- and intermolecular ether bond formation, attributed to photothermal degradation [35]. These findings suggest that the slight broadening of NMR peaks and reduction in crystallinity may be due to subtle changes, possibly resulting from photothermal decomposition rather than simple photochemical reactions. Therefore, while laser irradiation largely preserves the structure and bonding in CNF, it is inferred that minor changes occur at the microstructural level.

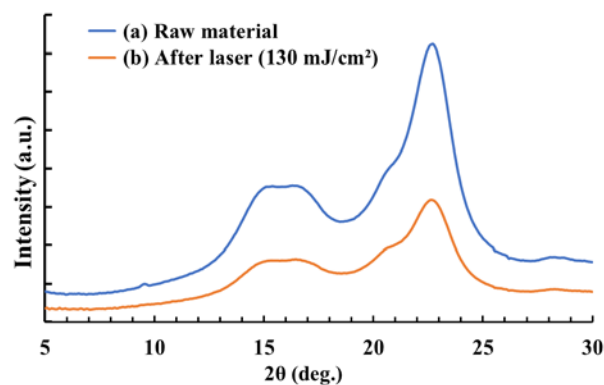


Fig. 7 XRD profiles of CNFs from (a) raw material and (b) after laser irradiation with 130 mJ/cm².

3.4 LCNF

SEM images of LCNF before and after laser irradiation are displayed in Fig. 8. Lignin attached to the CNFs was observed. After five hours of laser irradiation, the lignin on the CNF appeared to be more finely dispersed, indicating that the lignin structure had been fragmented by laser irradiation.

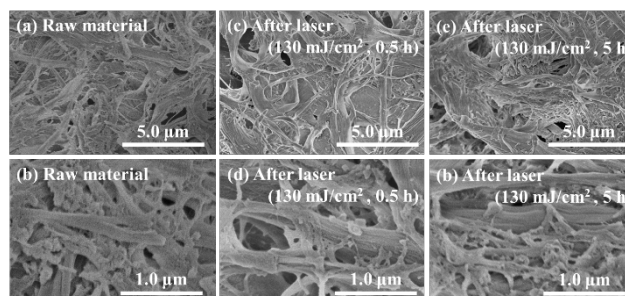


Fig. 8 SEM images of LCNF at (a) low and (b) high magnification with raw materials, (c) low and (d) high magnification after 0.5 h of laser irradiation at 130 mJ/cm², and (e) low and (f) high magnification after 5 h of laser irradiation, respectively.

Subsequently, the results of the ^{13}C solid NMR measurements on LCNF before and after laser irradiation are presented in Fig. 9. All peaks were attributed to either cellulose or lignin [38-40]. Peaks were noted around 20 ppm for $-\text{CH}_3$, 55 ppm for $-\text{OCH}_3$ in lignin, 62-65 ppm for C6 in cellulose, 72-75 ppm for C2, 3, 5 in cellulose, 83 ppm for C4 in cellulose (amorphous), 88 ppm for C4 in cellulose (crystalline), 80-88 ppm for α , β and γ in lignin (guaiacyl ring), 105 ppm for C1 in cellulose, 120 ppm for C-H in C2, 5, 6 in lignin (guaiacyl ring), 138 ppm for C-C in C1 in lignin (guaiacyl ring), 148 ppm for C-O in C3, 4 in lignin (guaiacyl ring), and 172 ppm for carbonyl groups. No changes in the intensity of CNF-derived peaks were observed. In contrast, a decrease in the intensity of lignin-derived peaks (55, 85, 110-150 ppm) and an increase in the intensity of CH_3 and carbonyl group peaks (20-50, 172 ppm) were recorded. These changes suggested that lignin was decomposed by laser irradiation, and decomposition products such as quinone compounds were detected. A broad peak appeared between 30 and 50 ppm, likely corresponding to decomposition products containing carbon double bonds, such as methylene groups, formed by the cleavage of aromatic rings and α , β , γ bonds in lignin. It has been reported that quinone compounds are produced by 350 nm light irradiation of lignin model compounds [41].

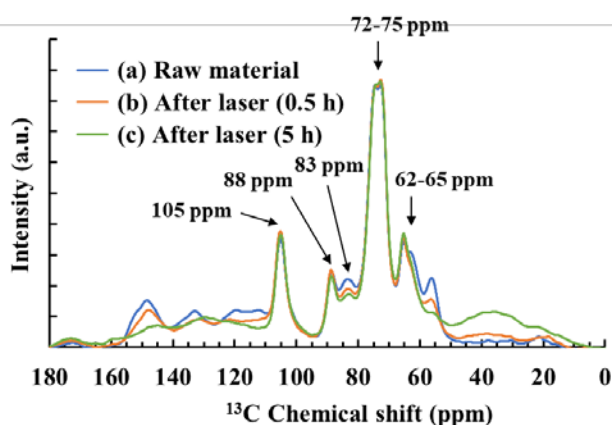


Fig. 9 ^{13}C solid NMR of LCNFs from (a) raw material and after laser irradiation with 130 mJ/cm^2 for (b) 0.5 h, (c) 5h, respectively.

The XRD results for CNF before and after laser irradiation are shown in Fig. 10. The diffraction patterns for the (200), (110), and (1-10) planes remained consistent before and after irradiation, indicating the presence of a cellulose I β structure. The crystalline was measured at 47.2 before irradiation, rising to 50.6 after 0.5 hours of laser exposure. This increase suggests that partial lignin decomposition raised the relative crystallinity by increasing the proportion of CNF. However, after 5 hours of laser irradiation, the crystallinity decreased to 44.4, likely due to a slight reduction in the crystallinity of the CNF itself with extended exposure, as seen in section 3.3.

Based on these results, laser irradiation of LCNF appears to induce photodegradation of lignin, producing quinone compounds and decomposition products containing carbon double bonds. In contrast, while the crystallinity of CNF slightly decreases, the overall structure remains unchanged.

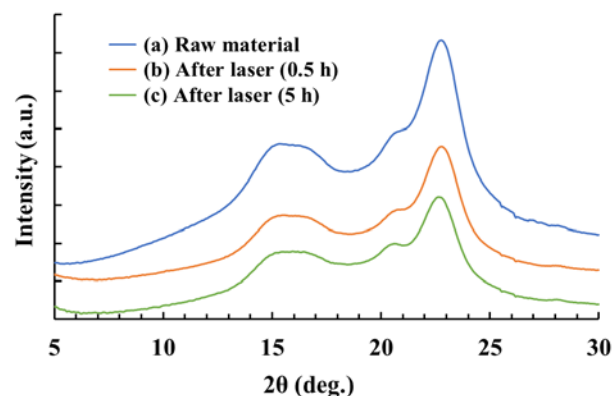


Fig. 10 XRD profiles of LCNFs from (a) raw material and after laser irradiation with 130 mJ/cm^2 for (b) 0.5 h, (c) 5h, respectively.

4. Conclusions

This study demonstrated a novel method for selectively decomposing lignin in lignocellulose nanofibers (LCNFs) using 355 nm laser irradiation, providing an eco-friendly alternative for cellulose nanofiber (CNF) production. Through extensive characterization, it was shown that while the laser irradiation effectively decomposed lignin into smaller fragments and products like quinone compounds, the CNF maintained its structural integrity. SEM and ^{13}C NMR analyses confirmed minimal CNF morphology and bonding changes, with only slight peak broadening due to minor structural adjustments. XRD analysis indicated a stable cellulose I β crystal structure, with only a modest reduction in crystallinity after prolonged irradiation, likely due to minor photothermal effects on the CNF.

These findings suggest that laser irradiation primarily affects lignin within LCNFs, enabling controlled decomposition while preserving the CNF structure. This highlights the potential for environmentally friendly CNF processing. Furthermore, the ability to precisely control irradiation conditions suggests that this method may also allow accurate adjustment of the component ratios in the final product. This study's limitations include further investigation into the impact of decomposition products, mechanical property evaluation, and scalability using larger sample quantities.

Acknowledgments

This work was supported by JST SPRING, Grant Number JPMJSP2106. The authors thank Materials Analysis Division, Core Facility Center, Institute of Science Tokyo.

References

- [1] H. Jørgensen, J. B. Kristensen, and C. Felby: *Biofuels, Bioprod. Bioref.*, 1, (2007) 119.
- [2] A. Isogai, T. Saito, and H. Fukuzumi: *Royal Soc. Chem.*, 3, (2011) 71.
- [3] T. Nishino, I. Matsuda, and K. Hirao: *Macromol.*, 37, (2004) 7683.
- [4] D. H. Page and F. E-Hosseiny: *J. Pulp Pap. Sci.*, 9, (1983) 99.
- [5] H. Yano, J. Sugiyama, A. N. Nakagaito, M. Nogi, T. Matsuura, M. Hikita, and K. Handa: *Adv. Mater.*, 17, (2005) 153.

- [6] M. Nogi, S. Iwamoto, A. N. Nakagaito, and H. Yano: *Adv. Mater.*, 21, (2009) 1595.
- [7] T. T. Nge, M. Nogi, and K. Suganuma: *J. Mater. Chem. C*, 1, (2013) 5235.
- [8] K. Nagashima, H. Koga, U. Celano, F. Zhuge, M. Kanai, S. Rahong, G. Meng, Y. He, J. D. Boeck, M. Jurczak, W. Vandervorst, T. Kitaoka, M. Nogi, and T. Yanagida: *Sci. Rep.*, 4, (2014) 1.
- [9] S. Ifuku, M. Nogi, K. Abe, K. Handa, F. Nakatsubo, and H. Yano: *Biomacromol.*, 8, (2007) 1973.
- [10] S. Fujisawa, T. Saito, S. Kimura, T. Iwata, and A. Isogai: *Biomacromol.*, 14, (2013) 1541.
- [11] A. Meftahi, P. Samyn, S. A. Geravand, R. Khajavi, S. Alibkhshi, M. Bechelany, and A. Barhoum: *Carbohydr. Polym.*, 278, (2022) 1.
- [12] H. Fukuzumi, T. Saito, T. Iwata, Y. Kumamoto, and A. Isogai: *Biomacromol.*, 10 (2009), 162.
- [13] M. Visanko, J. A. Sirvio, P. Piltanen, R. Sliz, H. Liimatainen, and M. Illikainen: *Cellul.*, 24, (2017) 4173.
- [14] J. A. Sirviö, M. Y. Ismail, K. Zhang, M. V. Tejesvi, and A. Ämmälä: *J. Mater. Chem. A*, 8, (2020) 7935.
- [15] J. A. Sirviö and M. Visanko: *J. Hazard. Mater.*, 383, (2020) 121174.
- [16] P. Kumar, D. M. Barrett, M. J. Delwiche, and P. Stroeve: *J. Am. Chem. Soc.*, 48 (2009), 3713.
- [17] Z. Jin, K. S. Katsumata, T. B. T. Lam, and K. Iiyama: *Biopolym.*, 83, (2006) 103.
- [18] M. Henriksson, L. A. Berglund, P. Isaksson, T. Lindström, and T. Nishino: *Biomacromol.*, 9, (2008) 1579.
- [19] S-H. Lee, Y. Teramoto, and T. End: *Compos.: Part A*, 42, (2011) 151.
- [20] L. Zhang, T. Tsuzuki, and X. Wang: *Cellul.*, 22, (2015) 1729.
- [21] W. Stelte and A. R. Sanadi: *Ind. Eng. Chem. Res.*, 48, (2009) 11211.
- [22] S. Zhang, A. Tanioka, M. Okamoto, Y. Haraoka, N. Hayashi, and H. Matsumoto: *ACS Appl. Polym. Mater.*, 2, (2020) 2830.
- [23] K. Abe, S. Iwamoto, and H. Yano: *Biomacromol.*, 8, (2007) 3276.
- [24] M. Pääkkö, M. Ankerfors, H. Kosonen, A. Nykänen, S. Ahola, M. Österberg, J. Ruokolainen, J. Laine, P. T. Larsson, O. Ikkala, and T. Lindström: *Biomacromol.*, 8 (2007), 1934.
- [25] L. Segal, J. J. Creely, A. E. Martin. Jr., and C. M. Conrad: *Textile Res. J.*, 29, (1959) 786.
- [26] R.L. Feller: "Accelerated Aging. Photochemical and Thermal Aspects" (The Getty Conservation Institute, Pasadena, 1994) p.47.
- [27] N-S. Hon: *J. Polym. Sci.: Polym. Chem. Ed.*, 13, (1975) 1347.
- [28] U. Müller, M. Rätzsch, M. Schwanninger, M. Steiner, and H. Zöbl: *J. Photochem. Photobiol. B*, 69, (2003) 97.
- [29] M. Takada, R. Niu, E. Minami, and S. Saka: *Biomass Bioenergy*, 115, (2018) 130.
- [30] H. Zhang, X. Wang, J. Wang, Q. Chen, H. Huang, L. Huang, S. Cao, and X. Ma: *J. Wood Sci. Technol.*, 54, (2020) 837.
- [31] T. Bikova and A. Treimanis: *Carbohydr. Polym.*, 55, (2004) 315.
- [32] E. Dorrestijn: *J. Anal. Appl. Pyrol.*, 54, (2000) 153.
- [33] Z. Jin, K. S. Katsumata, T. B. T. Lam, and K. Iiyama: *Biopolym.*, 83, (2006) 103.
- [34] Ö. Eriksson, D. A. I. Goring, and B. O. Lindgren: *Wood Sci. and Technol.*, 14, (1980) 267.
- [35] C. Assor, V. Placet, B. Chabbert, A. Habrant, C. Lapiere, B. Pollett, and P. Perre: *J. Agric. Food Chem.*, 57, (2009) 6830.
- [36] T. Iwara and L. Indrarti, J. Azuma, *Cellul.*, 5, (1998) 215.
- [37] H. Kono, S. Yunoki, T. Shikano, M. Fujiwara, T. Erata, and M. Taka: *J. Am. Chem. Soc.*, 124, (2002) 7506.
- [38] S. G. Kostryukov, P. S. Petrov, Yu. Yu. Masterova, T. D. Idris, S. S. Hamdamov, I. A. Yunusov, and N. S. Kostryukov: *Russ. J. Bioorg. Chem.*, 48, (2022) 1441.
- [39] M. M. Hossain, A. Rawal, and L. Aldous: *ACS Sustainable Chem. Eng.*, 7, (2019) 11928.
- [40] A. Teleman, P. T. Larsson, and T. Iversen: *Cellul.*, 8, (2001) 209.
- [41] O. Lanzaunga and M. Bietti: *J. photochem. photobiol., B Biol.*, 56, (2000) 85.

(Received: November 6, 2024, Accepted: April 30, 2025)